JOURNAL OF MASS SPECTROMETRY
*J. Mass Spectrom.* 2007; **42**: 918–928

JMS

# Electrospray ionization-multistage tandem mass spectrometry of complex multitin organometallic compounds

**Robert Jirásko,[1] Michal Holčapek,[1]* Lenka Kolářová[1] and Tushar S. Basu Baul[2]**

[1] Department of Analytical Chemistry, Faculty of Chemical Technology, University of Pardubice, nám. Čs. legií 565, 53210 Pardubice, Czech Republic
[2] Department of Chemistry, North-Eastern Hill University, NEHU Permanent Campus, Umshing, 793 022, Shillong, India

Received 15 March 2007; Accepted 11 April 2007

**The series of 14 complex organotin(IV) compounds containing many tin atoms and noncovalent bonds in the structure was characterized by electrospray ionization multistage tandem mass spectrometry (ESI-MS$^n$). The mass spectra were measured in both polarity modes to obtain complementary structural information. The characteristic pattern of ten natural tin isotopes allowed the determination of the number of tin atoms in the molecular adducts and fragment ions by comparing theoretical and experimental isotopic distributions. Positive ion ESI spectra show unusual adduct formation depending on the type of organic solvent used for the direct infusion analysis owing to the ion–molecule reactions in the ion source. On the basis of the detailed spectral interpretation of organotin(IV) compounds, the fragmentation patterns of multitin organometallic compounds have been proposed. Noncovalent bonds in polymeric complexes are fragmented first, which is then followed by characteristic neutral losses in monomeric units. Copyright © 2007 John Wiley & Sons, Ltd.**

**KEYWORDS:** electrospray; organotin; organometallics; speciation; adduct; ion trap

## INTRODUCTION

Organotin(IV) compounds play an important role in current research owing to their potential antitumor activity and catalytic properties.[1–3] These compounds are used in industrial processes, for example, as catalysts and stabilizers of rigid polyvinyl chloride.[4,5] Organotin(IV) compounds are also commonly used in agriculture, such as in fungicides, insecticides and biocides.[4,6]

Currently, a large number of new organotin(IV) compounds are being synthesized and their biological applications evaluated. For these reasons, a reliable, fast and inexpensive analytical technique is needed for the structure characterization and also for the monitoring the reaction pathways.[7–9] Several spectral techniques are available for this purpose[10–14] and one of the established methods used for the structure elucidation of organotin(IV) compounds is nuclear magnetic resonance (NMR) based on $^{1}$H, $^{13}$C and $^{119}$Sn chemical shifts.[15–18] On the other hand, a powerful technique such as X-ray crystallography is the method of choice[19–21] for the ultimate structure characterization, but it requires a single crystal which is difficult to obtain. In the past, mass spectrometry (MS) was used only for rather simple low-mass organotin(IV) compounds because of the volatility limitation of conventional electron ionization. However, electrospray ionization (ESI) MS, as the softest available ionization technique, can be applied for various organic, bioorganic and organometallic compounds having polar to ionic character, high molecular weights (MWs) and also noncovalent bonds.[7,9,22–29]

Polyisotopic elements have a characteristic distribution of isotopic peaks, which may help in the interpretation of mass spectra.[30–32] According the characteristic tin isotopic pattern with ten naturally occurring isotopes, it is possible to determine the number of tin atoms, in particular ions, on the basis of the comparison of theoretical and experimental isotopic distributions. The interpretation of mass spectra of complex organotin(IV) compounds is often difficult because noncovalent bonds of these compounds can be cleaved easily during the ionization process and therefore the molecular adducts missing completely, or because their relative abundances are very low or negligible in the full-scan mass spectra.[10] Further, the adduct formation with some solvents may complicate the interpretation of the mass spectra.[9,15]

In this work, complex multitin organometallic compounds have been studied using ESI-MS$^n$ analysis. Mass spectra have been interpreted in detail and the fragmentation patterns proposed. The characteristic isotopic distribution of tin atom has been used for the determination of the number of tin atoms by comparison of theoretical and experimental isotopic distributions. Finally, the adduct formation with different solvents (acetonitrile, methanol, ethanol and 2-propanol) has been studied in the positive ion mode for seven organotin(IV) compounds.

---

*Correspondence to: Michal Holčapek, Department of Analytical Chemistry, Faculty of Chemical Technology, University of Pardubice, nám. Čs. legií 565, 53210 Pardubice, Czech Republic.
E-mail: Michal.Holcapek@upce.cz

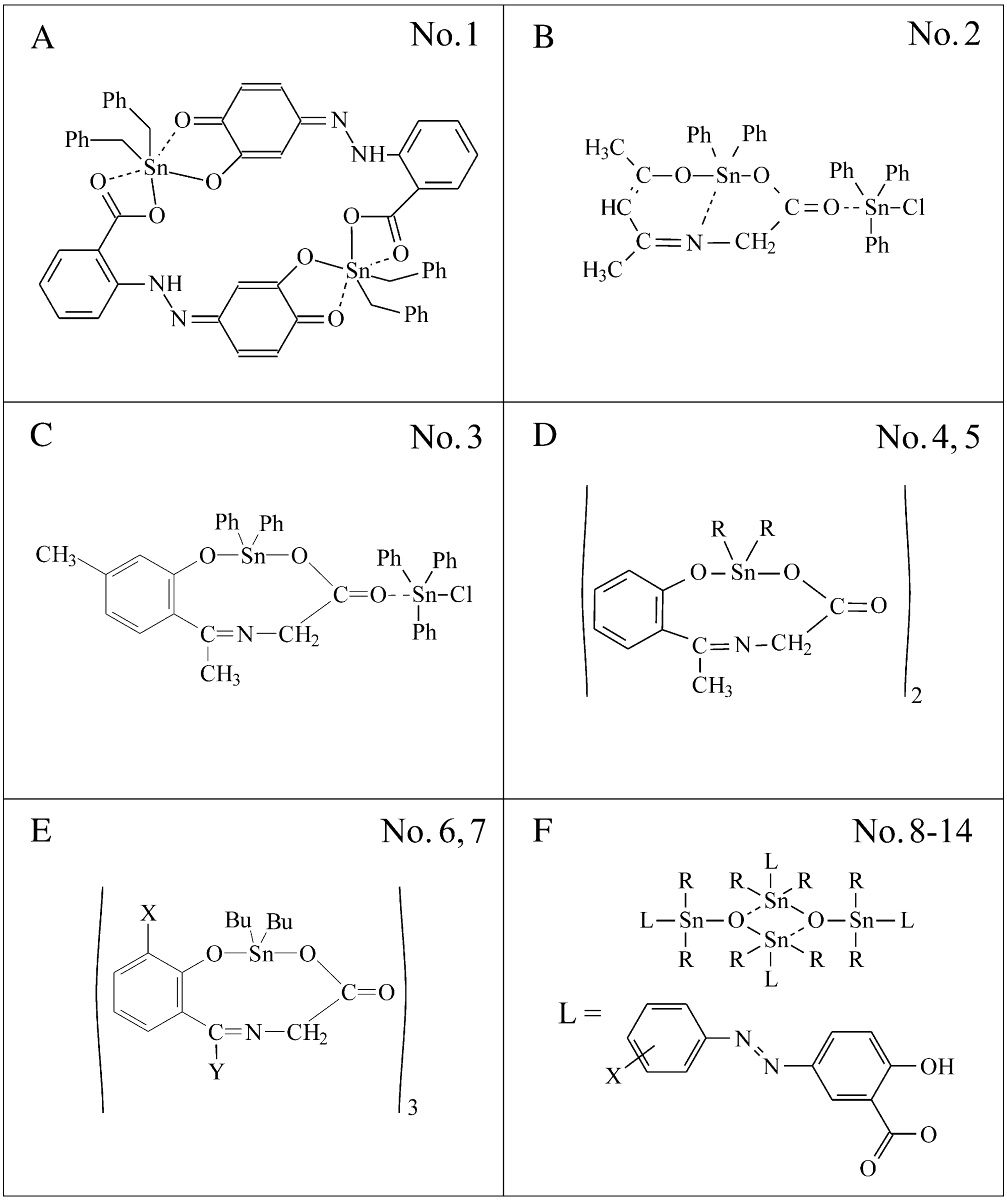

**Figure 1.** Structures of studied organotin(IV) compounds: (A) **1**; (B) **2**; (C) **3**; (D) **4** (R = $CH_3$), **5** (R = butyl); (E) **6** (X = H, Y = H), **7** (X = $CH_3$, Y = $CH_3$); (F) **8** (R = butyl, X = Cl), **9** (R = butyl, X = Br), **10** (R = butyl, X = H), **11** (R = butyl, X = $CH_3$), **12** (R = octyl, X = H), **13** (R = octyl, X = Cl), **14** (R = octyl, X = $OCH_3$).

## EXPERIMENTAL

### Organotin(IV) compounds

All organotin(IV) compounds (**1**–**14**) studied in this work (Fig. 1) were synthesized[10,12,33] at the North-Eastern Hill University, Umshing, Shillong, India. The structures were previously confirmed by $^1H$, $^{13}C$ and $^{119}Sn$ NMR spectra and in some cases by X-ray diffraction measurements in the solid state.[10,12,33]

### Instrumentation

The ESI mass spectra were measured on an Esquire 3000 ion trap instrument (Bruker Daltonics, Bremen, Germany). The samples were dissolved in acetonitrile or methanol. In addition, the samples **8**–**14** were also dissolved in ethanol and 2-propanol to study the formation of adduct ions. The samples were analyzed by direct infusion at the flow rate of 5 μl/min. Mass spectra were recorded in the range $m/z$ 50–2600 both in positive and negative ion modes. The selected precursor ions were further analyzed using MS$^n$ analyses under the following conditions: isolation width of $m/z$ 8 (or $m/z$ 12 for ions containing more tin atoms), collision amplitude of 0.8–1 V depending on the ion stability, ion source temperature of 300 °C, and flow rate and pressure of nitrogen of 4 l/min and 10 psi, respectively. The value of tuning parameter 'compound stability' was 100% and sometimes this parameter was reduced to 20% to avoid undesirable fragmentation in the ion source (see 'Results and discussion').

### ESI mass spectra

Ions observed in the full-scan positive and negative ion ESI mass spectra are listed bellow. The following symbols are used throughout the paper: Ph (phenyl, $C_6H_5$), benzene ($C_6H_6$), Bu (butyl, $C_4H_9$), butane ($C_4H_{10}$), butene ($C_4H_8$),

DOI: 10.1002/jms

Bz (benzyl, $CH_2C_6H_5$) and toluene ($CH_3C_6H_5$). All $m/z$ values are related to the most abundant natural isotopes, i.e. $^{120}$Sn isotope for tin atoms.

### *Compound **1**, MW($C_{54}H_{44}O_8N_4Sn_2$) = 1116.1 Da (Fig. 1(A))*

Positive ion mass spectra: $m/z$ 1155 $[M + K]^+$; $m/z$ 1139 $[M + Na]^+$, 100%; $m/z$ 597 $[M_{mono} + K]^+$; $m/z$ 581 $[M_{mono} + Na]^+$. MS/MS of $m/z$ 1155: $m/z$ 973 $[M + K - 2 \times Bz]^+$; $m/z$ 791 $[M + K - SnBz_2 - H_2O - CO_2]^+$; $m/z$ 597 $[M_{mono} + K]^+$; $m/z$ 415 $[M_{mono} + K - 2 \times Bz]^+$. MS/MS of $m/z$ 1139: $m/z$ 1047 $[M + Na - \text{toluene}]^+$; $m/z$ 955 $[M + Na - 2 \times \text{toluene}]^+$; $m/z$ 937 $[M + Na - 2 \times \text{toluene} - H_2O]^+$; $m/z$ 773 $[M + Na - 2\times \text{toluene} - 2 \times Bz]^+$; $m/z$ 671 $[M + Na - \text{toluene} - 376]^+$; $m/z$ 581 $[M_{mono} + Na]^+$; $m/z$ 489 $[M_{mono} + Na - \text{toluene}]^+$; $m/z$ 399 $[M_{mono} + Na - 2 \times Bz]^+$. MS/MS of $m/z$ 597: $m/z$ 415 $[M_{mono} + K - 2 \times Bz]^+$. MS/MS of $m/z$ 581: $m/z$ 399 $[M_{mono} + Na - 2 \times Bz]^+$.

**Table 1.** The list of ions observed in full-scan mass spectra of compounds **8–14** measured in different solvents (acetonitrile, methanol, ethanol and 2-propanol). Numbers in the table correspond to numbers of studied compounds according to Fig. 1. Suggested structures of observed adduct (A) and fragment (F) ions are shown in Fig. 7

| Ion | Acetonitrile | Methanol | Ethanol | 2-Propanol |
|---|---|---|---|---|
| Fragment ion $F_1$ | **14** | **8–14** | **12; 14** | – |
| Fragment ion $F_2$ | **8–11** | – | **8–11** | **8–12; 14** |
| Fragment ion $F_3$ | **8–14** | **8–11** | **8–14** | **8–14** |
| Fragment ion $F_4$ | **8–14** | | **8–14** | **8–14** |
| Adduct ion $A_1$ | **8–11** | **8–11** | **8–14** | **8–14** |
| Adduct ion $A_2$ | **8–12; 14** | – | **8–12** | **8–11** |
| Adduct ion $A_3$ | **12; 14** | – | **8–12** | **8–14** |
| Adduct ion $A_4$ | **8–11** | **8; 10** | **8–14** | **8–14** |
| Adduct ion $A_5$ | **8–11** | **8–11** | **8–14** | **9–14** |
| Adduct ion $A_6$ | **8–14** | **8–14** | **8–14** | **8–14** |
| Adduct ion $A_7$ | **10; 11** | – | **8–14** | **8–14** |
| Adduct ion $A_8$ | – | – | **8–14** | **8–14** |

Negative ion mass spectra: $m/z$ 1137 $[M + Na - 2H]^-$; $m/z$ 1115 $[M - H]^-$; $m/z$ 933 $[M - H - 2 \times Bz]^-$; $m/z$ 723 $[M - SnBz_3]^-$; $m/z$ 557 $[M_{mono} - H]^-$; $m/z$ 257 $[M_{mono} - HSn(CH_2C_6H_4)_2]^-$, 100%; $m/z$ 213 $[M_{mono} - HSn(CH_2C_6H_4)_2 - CO_2]^-$. MS/MS of $m/z$ 1137: $m/z$ 953 $[M + Na - 2H - 2 \times \text{toluene}]^-$; $m/z$ 771 $[M + Na - 2H - 2 \times \text{toluene} - 2 \times Bz]^-$; $m/z$ 727 $[M + Na - 2H - 2 \times \text{toluene} - 2 \times Bz - CO_2]^-$. MS/MS of $m/z$ 1115: $m/z$ 933 $[M - H - 2 \times Bz]^-$; $m/z$ 751 $[M - H - 4 \times Bz]^-$; $m/z$ 723 $[M - SnBz_3]^-$; $m/z$ 557 $[M_{mono} - H]^-$. MS/MS of $m/z$ 933: $m/z$ 751 $[M - H - 4 \times Bz]^-$; $m/z$ 707 $[M - H - 4 \times Bz - CO_2]^-$; $m/z$ 557 $[M_{mono} - H]^-$. MS/MS of $m/z$ 723: $m/z$ 679 $[M - SnBz_3 - CO_2]^-$; $m/z$ 633 $[M - HSnBz_2 - 2 \times CH_3C_6H_3]^-$; $m/z$ 257 $[M_{mono} - HSn(CH_2C_6H_4)_2]^-$; $m/z$ 213 $[M_{mono} - HSn(CH_2C_6H_4)_2 - CO_2]^-$. MS/MS of $m/z$ 557: $m/z$ 513 $[M_{mono} - H - CO_2]^-$. MS/MS of $m/z$ 257: $m/z$ 213 $[M_{mono} - HSn(CH_2C_6H_4)_2 - CO_2]^-$.

### *Compound **2**, MW($C_{37}H_{34}O_3NSn_2Cl$) = 815.0 Da (Fig. 1(B))*

Positive ion mass spectra: $m/z$ 881 $[M_{di} + Na]^+$; $m/z$ 780 $[M - Cl]^+$, 100%; $m/z$ 468 $[M_{mono} + K]^+$; $m/z$ 452 $[M_{mono} + Na]^+$; $m/z$ 351 $[SnPh_3]^+$. MS/MS of $m/z$ 881: $m/z$ 452 $[M_{mono} + Na]^+$. MS/MS of $m/z$ 780: $m/z$ 351 $[SnPh_3]^+$. MS/MS of $m/z$

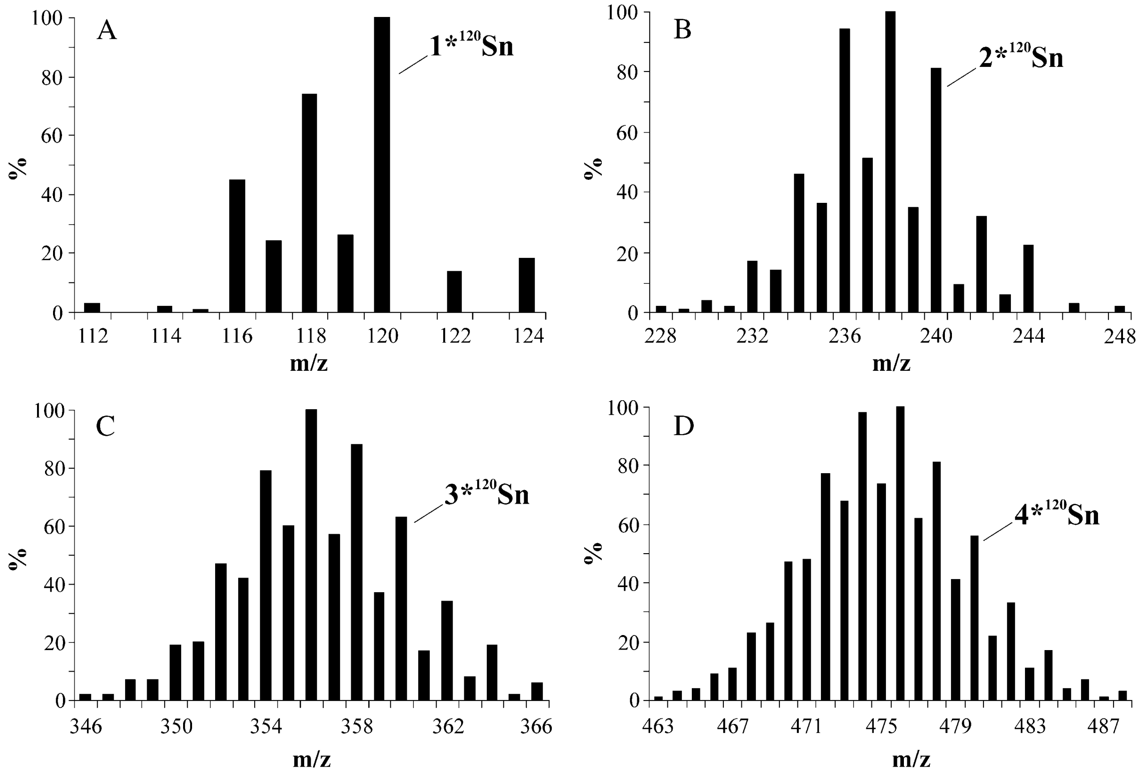

**Figure 2.** Theoretical isotopic abundances of ions containing: (A) one, (B) two, (C) three or (D) four tin atoms. The most abundant natural isotope is $^{120}$Sn.

DOI: 10.1002/jms

468: *m/z* 386 $[M_{mono} + K - CH_3COCH_2CCH]^+$. MS/MS of *m/z* 452: *m/z* 370 $[M_{mono} + Na - CH_3COCH_2CCH]^+$ ; *m/z* 134 $[M_{mono} + Na - SnPh_2 - CO_2]^+$.

Negative ion mass spectra: *m/z* 428 $[M_{mono} - H]^-$, 100%. MS/MS of *m/z* 428: *m/z* 384 $[M_{mono} - H - CO_2]^-$; *m/z* 306 $[M_{mono} - H - CO_2 - \text{benzene}]^-$; *m/z* 154 $[M_{mono} - H - SnPh_2]^-$.

### *Compound* **3**, *MW*($C_{41}H_{36}O_3NSn_2Cl$) = *865.0 Da (Fig. 1(C))*

Positive ion mass spectra: *m/z* 1476 $[M_{tri} + K]^+$; *m/z* 1460 $[M_{tri} + Na]^+$; *m/z* 997 $[M_{di} + K]^+$; *m/z* 981 $[M_{di} + Na]^+$; *m/z* 959 $[M_{di} + H]^+$; *m/z* 830 $[M - Cl]^+$; *m/z* 518 $[M_{mono} + K]^+$; *m/z* 502 $[M_{mono} + Na]^+$; *m/z* 480 $[M_{mono} + H]^+$, 100%. MS/MS of *m/z* 1460: *m/z* 981 $[M_{di} + Na]^+$. MS/MS of *m/z* 997: *m/z* 518 $[M_{mono} + K]^+$. MS/MS of *m/z* 982: *m/z* 502 $[M_{mono} + Na]^+$. MS/MS of *m/z* 959: *m/z* 480 $[M_{mono} + H]^+$; *m/z* 420 $[M_{mono} + H - CH_3COOH]^+$. MS/MS of *m/z* 830: *m/z* 351 $[SnPh_3]^+$. MS/MS of *m/z* 518: *m/z* 458 $[M_{mono} + K - CH_3COOH]^+$. MS/MS of *m/z* 502: *m/z* 442 $[M_{mono} + Na - CH_3COOH]^+$; *m/z* 297 $[SnPh_2 + Na]^+$. MS/MS of *m/z* 480: *m/z* 420 $[M_{mono} + H - CH_3COOH]^+$.

Negative ion mass spectra: *m/z* 478 $[M_{mono} - H]^-$, 100%; *m/z* 436 $[M_{mono} + Cl - \text{benzene}]^-$; *m/z* 397 $[Ph_2SnCl_3 + H_2O]^-$; *m/z* 197. MS/MS of *m/z* 478: *m/z* 434 $[M_{mono} - H - CO_2]^-$; *m/z* 356 $[M_{mono} - H - CO_2 - \text{benzene}]^-$; *m/z* 274 $[SnPh_2 - H]^{-\bullet}$ ; *m/z* 160 $[M_{mono} - H - CO_2 - SnPh_2]^-$. MS/MS of *m/z* 436: *m/z* 400 $[M_{mono} - H - \text{benzene}]^-$; *m/z* 356 $[M_{mono} - H - CO_2 - \text{benzene}]^-$. MS/MS of *m/z* 397: *m/z* 309 $[Ph_2SnCl]^-$.

### *Compound* **4**, *MW*($C_{24}H_{30}O_6N_2Sn_2$) = *682.0 Da (Fig. 1(D))*

Positive ion mass spectra: *m/z* 1365 $[M_{tetra} + H]^+$; *m/z* 721 $[M_{di} + K]^+$; *m/z* 705 $[M_{di} + Na]^+$, 100%; *m/z* 380 $[M_{mono} + K]^+$; *m/z* 364 $[M_{mono} + Na]^+$. MS/MS of *m/z* 1365: *m/z* 1024 $[M_{tri} + H]^+$; *m/z* 697. MS/MS of *m/z* 721: *m/z* 380 $[M_{mono} + K]^+$. MS/MS of *m/z* 705: *m/z* 364 $[M_{mono} + Na]^+$. MS/MS of *m/z* 364: *m/z* 320 $[M_{mono} + Na - CO_2]^+$; *m/z* 299.

Negative ion mass spectra: *m/z* 340 $[M_{mono} - H]^-$, 100%. MS/MS of *m/z* 340: *m/z* 312 $[M_{mono} - H - CO]^-$; *m/z* 296 $[M_{mono} - H - CO_2]^-$; *m/z* 205 $[(CH_3O)_2Sn + Na]^-$; *m/z* 146 $[M_{mono} - (CH_3)_2SnOCOH]^-$.

### *Compound* **5**, *MW*($C_{36}H_{54}O_6N_2Sn_2$) = *850.2 Da (Fig. 1(D))*

Positive ion mass spectra: *m/z* 1314 $[M_{tri} + K]^+$; *m/z* 1298 $[M_{tri} + Na]^+$, *m/z* 889 $[M_{di} + K]^+$; *m/z* 873 $[M_{di} + Na]^+$; 100%, *m/z* 464 $[M_{mono} + K]^+$; *m/z* 448 $[M_{mono} + Na]^+$; *m/z* 426 $[M_{mono} + H]^+$. MS/MS of *m/z* 1314: *m/z* 889 $[M_{di} + K]^+$; *m/z* 464 $[M_{mono} + K]^+$. MS/MS of *m/z* 1298: *m/z* 873 $[M_{di} + Na]^+$; *m/z* 448 $[M_{mono} + Na]^+$. MS/MS of *m/z* 889: *m/z* 464 $[M_{mono} + K]^+$. MS/MS of *m/z* 873: *m/z* 448 $[M_{mono} + Na]^+$. MS/MS of *m/z* 448: *m/z* 404 $[M_{mono} + Na - CO_2]^+$; *m/z* 334 $[M_{mono} + Na - \text{butene} - \text{butane}]^+$.

Negative ion ESI mass spectra: *m/z* 424 $[M_{mono} - H]^-$, 100%. MS/MS of *m/z* 424: *m/z* 310 $[M_{mono} - H - \text{butene} - \text{butane}]^-$; *m/z* 146 $[M_{mono} - H - SnBu_2 - CO_2]^-$.

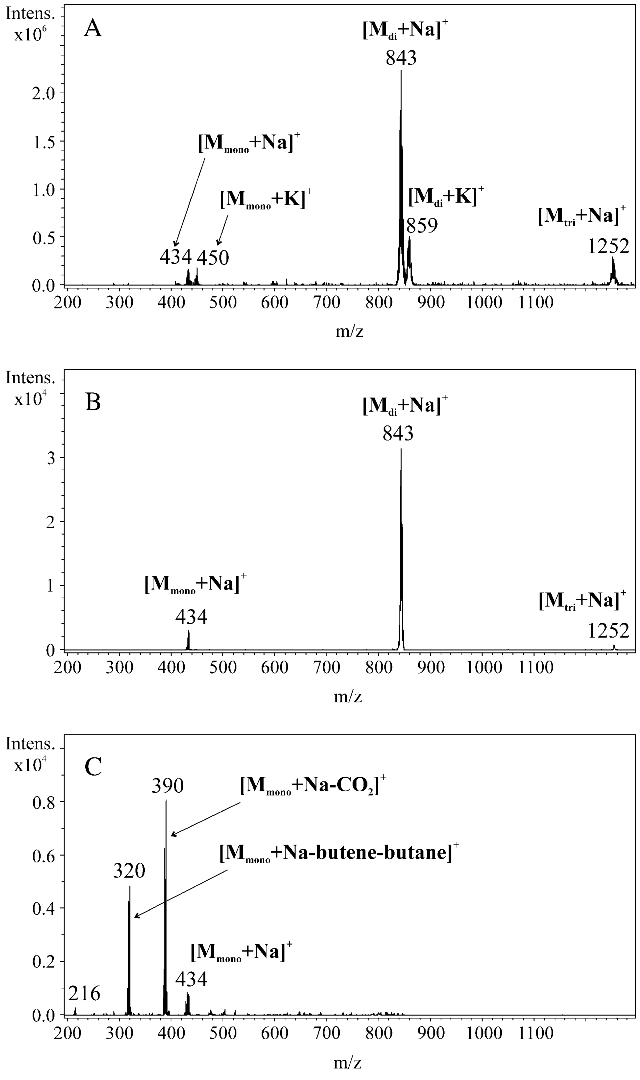

**Figure 3.** Positive ion ESI mass spectra of compound **6** (fragmentation pattern is shown in Fig. 5). The *m/z* values in this figure correspond to the most abundant isotopic peaks, which differ from the monoisotopic peak related to $^{120}Sn$ by two units for dimeric ions and by four units for trimeric ions. (A) full-scan mass spectrum, (B) MS/MS spectrum of the $[M_{tri} + Na]^+$ ion at *m/z* 1256, (C) MS/MS spectrum of $[M_{mono} + Na]^+$ ion at *m/z* 434.

### *Compound* **6**, *MW*($C_{51}H_{75}O_9N_3Sn_3$) = *1233.3 Da (Fig. 1(E))*

Positive ion mass spectra: *m/z* 1256 $[M_{tri} + Na]^+$; *m/z* 861 $[M_{di} + K]^+$; *m/z* 845 $[M_{di} + Na]^+$, 100%; *m/z* 450 $[M_{mono} + K]^+$; *m/z* 434 $[M_{mono} + Na]^+$. MS/MS of *m/z* 1256: *m/z* 845 $[M_{di} + Na]^+$; *m/z* 434 $[M_{mono} + Na]^+$. MS/MS of *m/z* 861: *m/z* 450 $[M_{mono} + K]^+$. MS/MS of *m/z* 845: *m/z* 434 $[M_{mono} + Na]^+$. MS/MS of *m/z* 434: *m/z* 390 $[M_{mono} + Na - CO_2]^+$; *m/z* 320 $[M_{mono} + Na - \text{butene} - \text{butane}]^+$.

Negative ion mass spectra: *m/z* 468 $[M_{mono} - H + \text{butane}]^-$; *m/z* 442 $[M_{mono} - H + CH_3OH]^-$; *m/z* 410 $[M_{mono} - H]^-$, 100%; *m/z* 358 $[M_{mono} - H - 2 \times \text{butane} + 2 \times CH_3OH]^-$; *m/z* 239 $[(CH_3O)_2SnBu]^-$; *m/z* 213 $[(CH_3O)_3Sn]^-$. MS/MS of *m/z* 468: *m/z* 354 $[M_{mono} - H - \text{butene}]^-$; *m/z* 310 $[M_{mono} - H - \text{butene} - CO_2]^-$. MS/MS of *m/z*

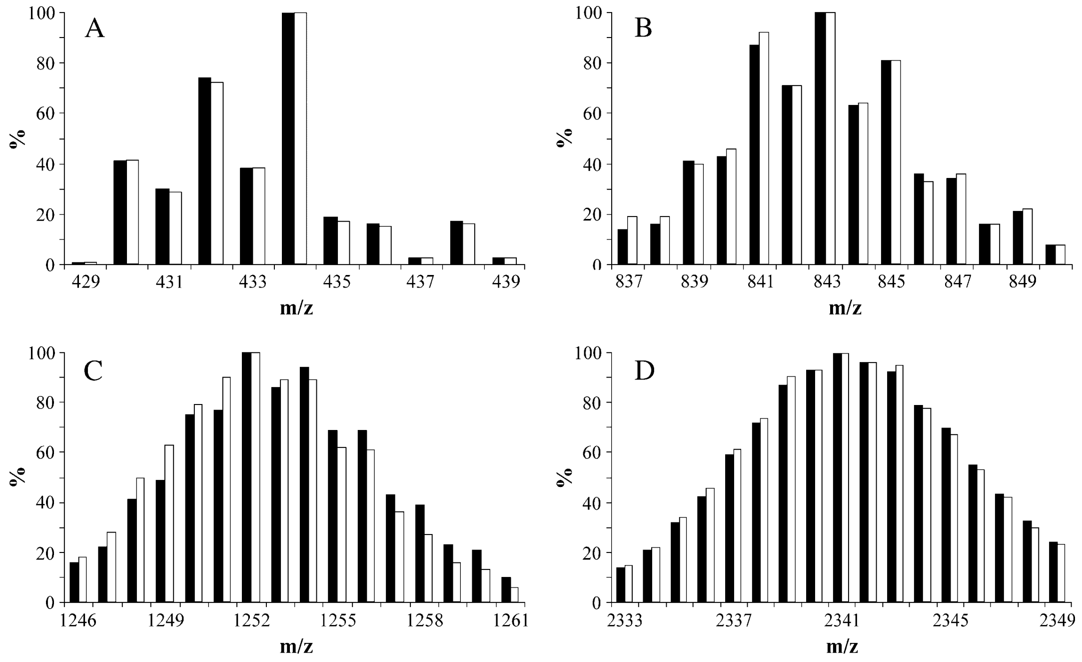

**Figure 4.** Comparison of experimental (white bars) and theoretical (black bars) isotopic abundances of ions with the different number of Sn atoms for compound **6**: (A) $[M_{mono} + Na]^+$ ion at *m/z* 434 with one Sn atom, (B) $[M_{di} + Na]^+$ ion at *m/z* 845 with two Sn atoms, (C) $[M_{tri} + Na]^+$ ion at *m/z* 1256 with three Sn atoms, and for compound **12**: (D) $[4 \times M_{mono} + Na]^+$ ion at *m/z* 2345 with four Sn atoms.

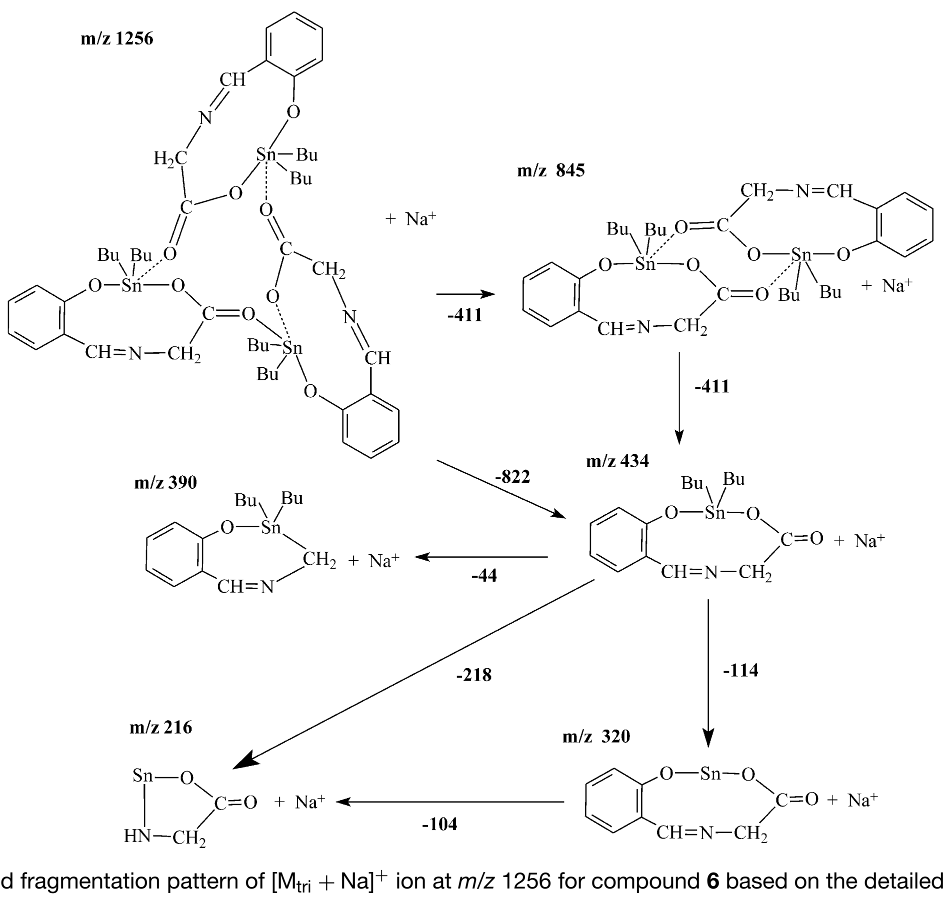

**Figure 5.** Suggested fragmentation pattern of $[M_{tri} + Na]^+$ ion at *m/z* 1256 for compound **6** based on the detailed interpretation of ESI-MS$^n$ spectra.

410: *m/z* 296 $[M_{mono} - H - \text{butene} - \text{butane}]^-$; *m/z* 132 $[M_{mono} - H - SnBu_2 - CO_2]^-$. MS/MS of *m/z* 358: *m/z* 326 $[M_{mono} - H - 2^*\text{butane} + CH_3OH]^-$; *m/z* 282 $[M_{mono} - H - 2^*\text{butane} + CH_3OH - CO_2]^-$; *m/z* 250 $[M_{mono} - H - 2 \times \text{butane} - CO_2]^-$; *m/z* 176 $[M_{mono} - H - SnBu_2]^-$; *m/z* 132 $[M_{mono} - H - SnBu_2 - CO_2]^-$.

### *Compound* **7**, *MW*($C_{57}H_{87}O_9N_3Sn_3$) = *1317.4 Da (Fig. 1(E))*

Positive ion mass spectra: $m/z$ 1356 $[\mathrm{M_{tri}+K}]^+$; $m/z$ 1340 $[\mathrm{M_{tri}+Na}]^+$; $m/z$ 917 $[\mathrm{M_{di}+K}]^+$; $m/z$ 901 $[\mathrm{M_{di}+Na}]^+$, 100%; $m/z$ 879 $[\mathrm{M_{di}+H}]^+$; $m/z$ 478 $[\mathrm{M_{mono}+K}]^+$; $m/z$ 462 $[\mathrm{M_{mono}+Na}]^+$; $m/z$ 440 $[\mathrm{M_{mono}+H}]^+$. MS/MS of $m/z$ 1340: $m/z$ 901 $[\mathrm{M_{di}+Na}]^+$. MS/MS of $m/z$ 917: $m/z$ 478 $[\mathrm{M_{mono}+K}]^+$. MS/MS of $m/z$ 901: $m/z$ 462 $[\mathrm{M_{mono}+Na}]^+$. MS/MS of $m/z$ 462: $m/z$ 348 $[\mathrm{M_{mono}+Na-butene-butane}]^+$.

Negative ion mass spectra: $m/z$ 438 $[\mathrm{M_{mono}-H}]^-$, 100%; $m/z$ 353 $[\mathrm{Bu_2SnCl_2OCH_3+H_2O}]^-$. MS/MS of $m/z$ 438: $m/z$ 324 $[\mathrm{M_{mono}-H-butene-butane}]^-$; $m/z$ 160 $[\mathrm{M_{mono}-H-SnBu_2-CO_2}]^-$. MS/MS of $m/z$ 353: $m/z$ 323 $[\mathrm{Bu_2SnCl_2OCH_3+H_2O-HCOH}]^-$; $m/z$ 265 $[\mathrm{Bu_2SnOCH_3}]^-$; $m/z$ 209 $[\mathrm{Bu_2SnOCH_3-butene}]^-$.

### *Compounds* **8–14** *(Fig. 1(F))*

The fragment and adduct ions observed in the full-scan positive ion ESI mass spectra of compounds **8**–**14** are summarized in Table 1. Calculated molecular formulas and molecular weights are the following: **8** – MW($C_{84}H_{104}O_{14}N_8Cl_4Sn_4$) = 2068.3 Da; **9** – MW($C_{84}H_{104}O_{14}N_8Br_4Sn_4$) = 2244.1 Da; **10** – MW($C_{84}H_{108}O_{14}N_8Sn_4$) = 1932.4 Da; **11** – MW($C_{88}H_{116}O_{14}N_8Sn_4$) = 1988.5 Da, **12** – MW($C_{116}H_{172}O_{14}N_8Sn_4$) = 2380.9 Da, **13** – MW($C_{116}H_{168}O_{14}N_8Cl_4Sn_4$) = 2516.8 Da, and **14** – MW($C_{120}H_{180}O_{18}N_8Sn_4$) = 2500.9 Da.

Negative ion ESI mass spectra of compounds **8**–**14** have the same pattern with the following types of ions: $[\mathrm{M-H+H_2O}]^-$; $[\mathrm{M-H}]^-$; $[3\times\mathrm{M_{mono}+L+LH}]^-$; $[3\times\mathrm{M_{mono}+L}]^-$; $[2\times\mathrm{M_{mono}+L+LH}]^-$; $[2\times\mathrm{M_{mono}+Cl+LH}]^-$; $[2\times\mathrm{M_{mono}+L}]^-$; $[2\times\mathrm{M_{mono}+Cl}]^-$; $[\mathrm{M_{mono}+L+LH}]^-$; $[\mathrm{M_{mono}+L+HCl}]^-$; $[\mathrm{M_{mono}+L}]^-$; $[\mathrm{M_{mono}+Cl}]^-$; $[\mathrm{L}]^-$, 100%; $[\mathrm{L-CO_2}]^-$.

## RESULTS AND DISCUSSION

Figure 1 shows the structures of the studied compounds, which had been already confirmed by X-ray diffraction and NMR spectroscopy in previous works.[10,12,33] These complex compounds containing two to four tin atoms are measured by ESI-MS in both polarity modes to obtain complementary information on their structures. Important ions are isolated in the ion trap and analyzed by subsequent MS$^n$ experiments to elucidate the ionic structure and also to characterize fragmentation patterns. A powerful tool in the interpretation of mass spectra of organotin(IV) compounds (especially those ions containing more tin atoms) is the characteristic natural isotopic pattern for tin atoms having ten isotopes, where $^{120}$Sn is the most abundant (Fig. 2(A)), but a more complex picture is obtained for ions containing two (Fig. 2(B)), three (Fig. 2(C)) or four (Fig. 2(D)) tin atoms. All masses listed in the 'Experimental' part and throughout the paper are related to all $^{120}$Sn configuration, but the most abundant ion correspond to the two mass units lower ion for two tin atoms or the four mass units lower ion for three and four tin atoms. This style of presentation seems to be the most suitable for avoiding the confusion during the calculation of masses of tin losses for multitin ions.

The studied compounds are divided into two groups in the following text. The first group (**1**–**7**) demonstrates the determination of the number of tin atoms, in particular ions and fragmentation patterns, while the second one (**8**–**14**) is used for experiments dealing with the adduct ion formation with different solvents.

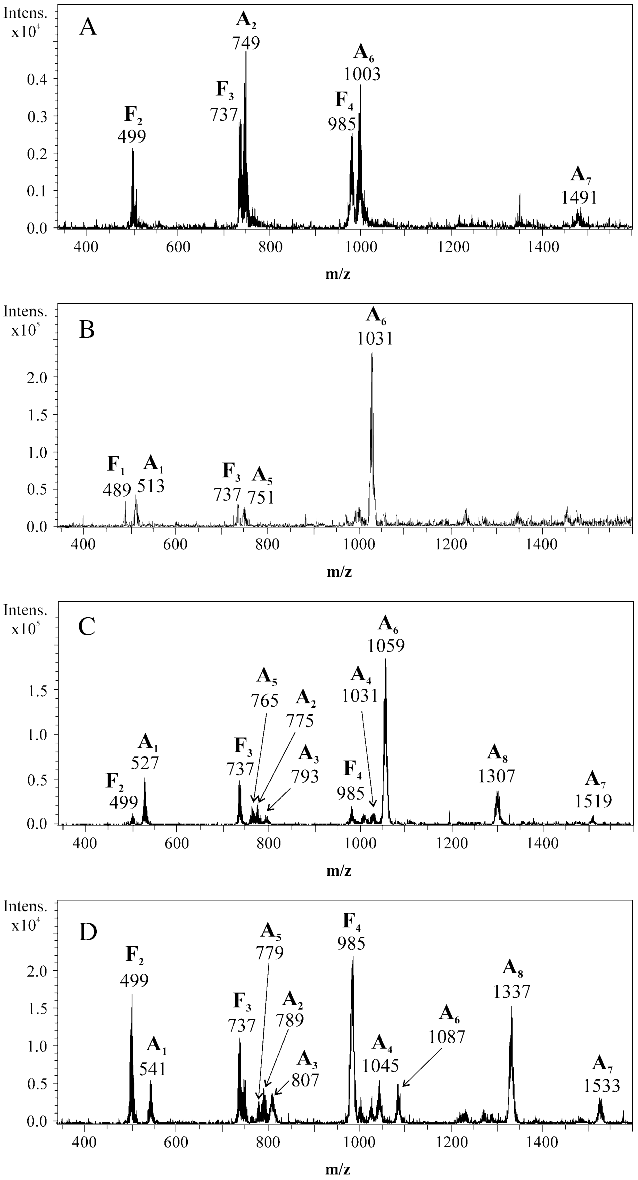

**Figure 6.** Positive ion ESI mass spectra of compound **11** measured in different solvents: (A) acetonitrile, (B) methanol, (C) ethanol, (D) 2-propanol. Structures of the observed ions and their symbols are shown in Fig. 7.

## Compounds 1–7

The presence of elements with abundant isotopes may somewhat complicate the determination of the number of tin atoms, but at least for one and two tin atoms the determination is straightforward. For more than two tin atoms, the isotopic abundances of other elements should be considered in the calculation, especially of those elements containing abundant isotopes, e.g. bromine and chlorine. The elemental composition of these polyisotopic compounds is verified by the comparison of the measured experimental isotopic distribution with the theoretically calculated distribution of the expected summary formula.

DOI: 10.1002/jms

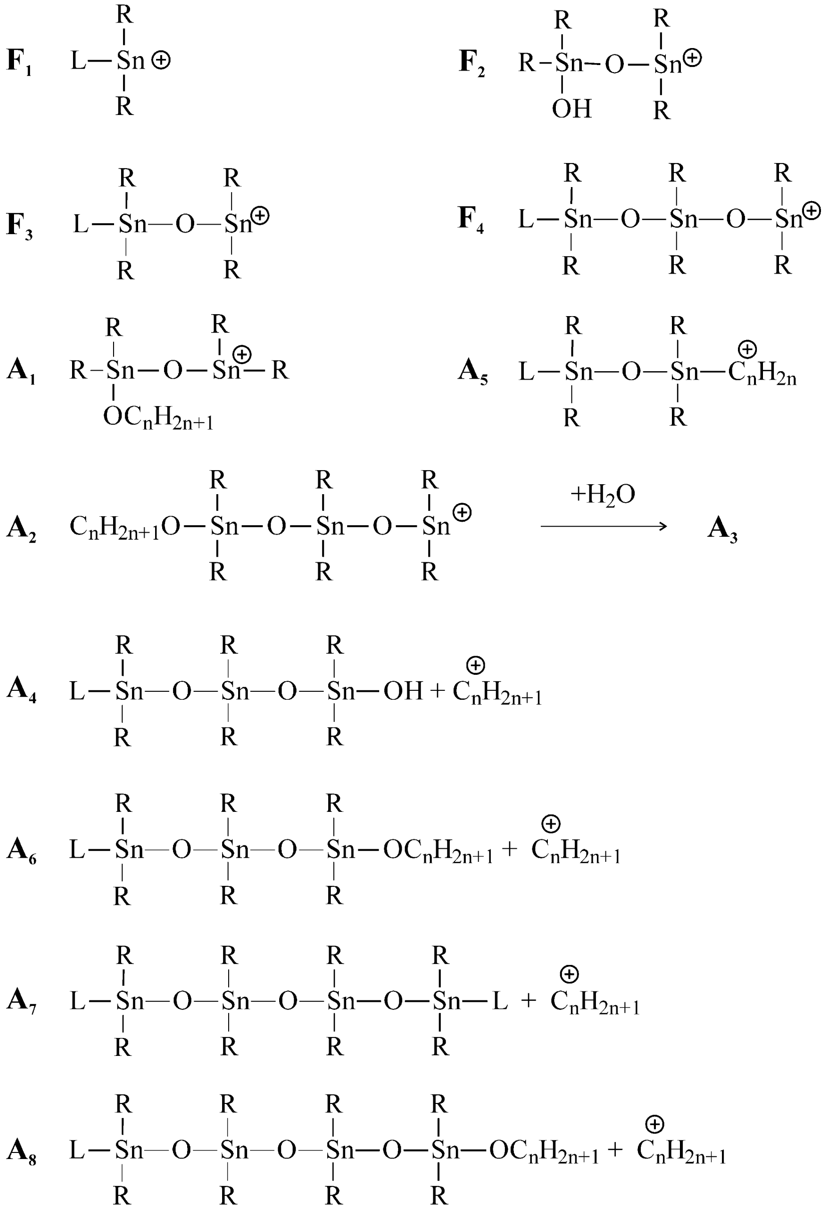

$$\mathbf{F_1}\quad L-\underset{R}{\overset{R}{Sn}}{}^{\oplus}$$

$$\mathbf{F_2}\quad R-\underset{OH}{\overset{R}{Sn}}-O-\underset{R}{\overset{R}{Sn}}{}^{\oplus}$$

$$\mathbf{F_3}\quad L-\underset{R}{\overset{R}{Sn}}-O-\underset{R}{\overset{R}{Sn}}{}^{\oplus}$$

$$\mathbf{F_4}\quad L-\underset{R}{\overset{R}{Sn}}-O-\underset{R}{\overset{R}{Sn}}-O-\underset{R}{\overset{R}{Sn}}{}^{\oplus}$$

$$\mathbf{A_1}\quad R-\underset{OC_nH_{2n+1}}{\overset{R}{Sn}}-O-\overset{R}{Sn}{}^{\oplus}-R$$

$$\mathbf{A_5}\quad L-\underset{R}{\overset{R}{Sn}}-O-\underset{R}{\overset{R}{Sn}}-\overset{\oplus}{C_nH_{2n}}$$

$$\mathbf{A_2}\quad C_nH_{2n+1}O-\underset{R}{\overset{R}{Sn}}-O-\underset{R}{\overset{R}{Sn}}-O-\underset{R}{\overset{R}{Sn}}{}^{\oplus}\xrightarrow{+H_2O}\mathbf{A_3}$$

$$\mathbf{A_4}\quad L-\underset{R}{\overset{R}{Sn}}-O-\underset{R}{\overset{R}{Sn}}-O-\underset{R}{\overset{R}{Sn}}-OH+\overset{\oplus}{C_nH_{2n+1}}$$

$$\mathbf{A_6}\quad L-\underset{R}{\overset{R}{Sn}}-O-\underset{R}{\overset{R}{Sn}}-O-\underset{R}{\overset{R}{Sn}}-OC_nH_{2n+1}+\overset{\oplus}{C_nH_{2n+1}}$$

$$\mathbf{A_7}\quad L-\underset{R}{\overset{R}{Sn}}-O-\underset{R}{\overset{R}{Sn}}-O-\underset{R}{\overset{R}{Sn}}-O-\underset{R}{\overset{R}{Sn}}-L+\overset{\oplus}{C_nH_{2n+1}}$$

$$\mathbf{A_8}\quad L-\underset{R}{\overset{R}{Sn}}-O-\underset{R}{\overset{R}{Sn}}-O-\underset{R}{\overset{R}{Sn}}-O-\underset{R}{\overset{R}{Sn}}-OC_nH_{2n+1}+\overset{\oplus}{C_nH_{2n+1}}$$

**Figure 7.** Suggested structures of observed fragment ions (F) and adduct ions (A) in full-scan, positive ion ESI mass spectra of compounds **8–14** (*n* is the number of carbon atoms in alcoholic solvent).

Our identification approach is demonstrated on the example of compound **6**. The mass spectrometric measurements of compounds containing noncovalent bonds are quite difficult. These bonds tend to fragment easily during the ionization process even under the softest ionization conditions, such as special setting of tuning parameters, where the parameter 'compound stability' is reduced from the default value 100% to 20% and some other transfer voltages are decreased manually to reduce the velocity and energy of the ions. The corresponding ions related to the MW determination (e.g. $[M+H]^+$, $[M-H]^-$ and some typical adduct ions) are often missing completely in the full-scan spectra of organometallic compounds. Unlike those of the common organic and bioorganic molecules typically containing only $[M+H]^+/[M-H]^-$ ions, the ESI mass spectra of mutlitin organometallic compounds are rather complex. The isotopic distributions of multitin ions are very broad, which result in decreased intensities of these high-mass ions because of the spreading of the total signal among many isotopic peaks. In some cases, the reduced value of tuning of the compound stability parameter to 20% improves signal-to-noise ratio. This setting of the compound stability parameter is used only for the measurement of positive ion mass spectra of compounds **1**, **4**, **5**, **6** and **7**. The ions providing information on MW are observed in the full-scan positive ion ESI mass spectra (see 'Experimental'); for example, the adduct with sodium ion is observed together with the fragment ions corresponding to sodium and potassium adducts with dimeric and monomeric ions in the full-scan positive ion mass spectrum of trimeric compounds **6** (Fig. 3(A)). The proposed structures of important ions observed in the spectra are confirmed by MS$^n$ analysis. The MS/MS spectrum of the most important $[M_{tri}+Na]^+$ ion at $m/z$ 1256 is shown in Fig. 3(B). Two subsequent losses of monomeric unit form dimeric and monomeric sodium adducts. The neutral loss of one monomeric unit is observed in MS$^3$ of

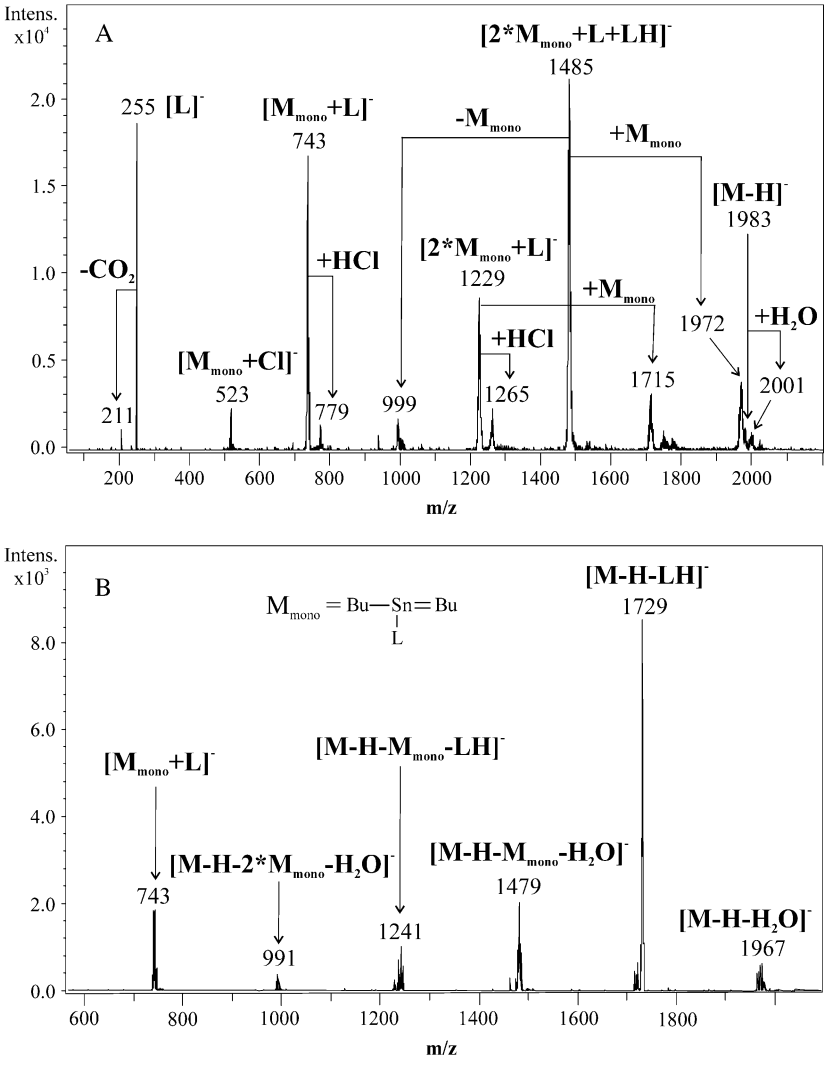

**Figure 8.** Negative ion ESI mass spectra of compound **11** measured in acetonitrile: (A) Full-scan mass spectrum, (B) MS/MS spectrum of the $[M - H]^-$ ion at $m/z$ 1987.

$[M_{di} + Na]^+$ ion at $m/z$ 843 (not shown). This observation confirms that the bonds among the monomeric units (noncovalent bonds) are much weaker compared to remaining covalent bonds, and hence the fragmentation of noncovalent bonds is strongly preferred. When all noncovalent bonds are broken, the fragmentation continues with covalent bonds, i.e. the fragmentation of monomeric species shown in Fig. 3(C). The characteristic neutral losses corresponding to the particular functional groups can be identified, such as $CO_2$ ($\Delta m/z$ 44, typical for organometallic carboxylates), butene ($\Delta m/z$ 56) or butane ($\Delta m/z$ 58) typical for the butyl substitution, and the neutral losses typical for phenyl substitution ($\Delta m/z$ 76 or 78), toluene ($\Delta m/z$ 90 or 92), etc. (for details, see 'Experimental').

In the negative ion mode, significantly better signal is observed when samples are dissolved in methanol instead of acetonitrile used for positive ion mode measurements. The deprotonated monomeric unit $[M_{mono} - H]^-$ is the base peak of all full-scan, negative ion spectra, which is very important for the confirmation of MW. The same results are observed also for the decreased value of the compound stability parameter to 20%. Contrary to the positive ion mode, the negative ion spectra do not provide any information on the polymeric species except for compound **1**, where the ions $[M - 2H + Na]^-$ at $m/z$ 1137 and $[M - H]^-$ at $m/z$ 1115 provide information on MW. Then, two similar monomeric units with $m/z$ 558 are formed by the cleavage of the most labile bond between Sn and O.

High signal averaging improves the precision of the comparison of experimental isotopic distributions with the theoretical ones used for the determination of the number of tin atoms in individual ions. This way the ratios of ions are stabilized. In this work, the following settings of tuning parameters is used: the target mass parameter is set to the value corresponding to $m/z$ value of precursor ion, the signal averaging is increased to $20 \times 10$ in comparison to standard values about $10 \times 2$. Averaging time is chosen 3–8 min depending on the signal stability and complexity of isotopic distribution. Theoretical distribution is calculated using the program IsoPro 3.0. Figure 4 shows satisfactory agreement between the experiment and theory for ions containing one (Fig. 4(A)), two (Fig. 4(B)), three (Fig. 4(C)) and four (Fig. 4(D)) Sn atoms. The interpretations of all MS and MS$^n$ spectra are combined, resulting in the final suggestion of fragmentation scheme (Fig. 5).

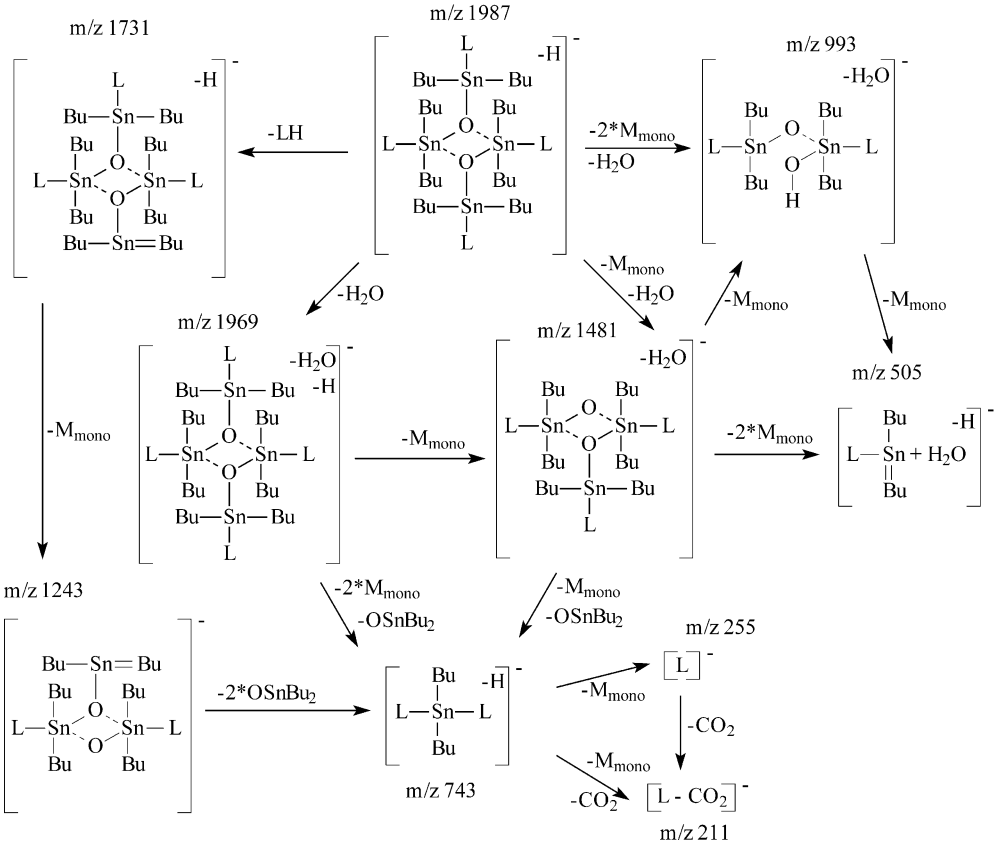

**Figure 9.** Suggested fragmentation pattern of the [M − H]$^-$ ion at *m/z* 1987 based on ESI-MS$^n$ analysis of compound **11**.

## Compounds 8–14

These compounds differ in the type of the substituent X on the ligand L and alkyl substitution R on the Sn atom (Fig. 1). For all compounds, the full-scan and MS$^n$ spectra are measured in both polarity modes, and the spectra are interpreted in detail with the emphasis on the correlation of the observed ions and structures. The complexity of isotopic distributions of polyisotopic compounds makes difficult the interpretation of their mass spectra. Therefore, the same approach is applied as discussed in previous paragraph. Moreover, the formation of unusual adduct ions with solvents is observed for this class of compounds. The formation of solvent adducts is observed only in the positive ion mode. To fully characterize these adducts, four solvents (acetonitrile, methanol, ethanol and 2-propanol) were selected in this study. An example of full-scan positive ion mass spectra of compound **11** measured subsequently in all solvents is shown in Fig. 6. The structures of the observed fragment (F) and adduct (A) ions are explained in Fig. 7. In general, similar types of ions are formed for all compounds and solvents but with different masses owing to the shifts of masses of individual solvents. Without the proper understanding of the adduct formation, one can hardly identify that the spectra presented in Fig. 6 correspond to a single compound.

The adduct ions have a polymeric character consisting of $OSnR_2$ (R = Bu or Oct) as a monomeric unit. In addition to the polymeric character, the spectra measured in alcoholic solvents also contain adducts with the alkyl ion coming from the alcohol unlike the measurements in acetonitrile, where the parameter $n$ ($n$ = number of carbon atoms in alcoholic solvent) is equal to zero. In case of acetonitrile, only adducts with $OSnR_2$ are observed in the spectra in contrast to alcoholic solvents. The lowest number and also lowest relative abundances of adduct ions are counted for methanol, while ethanol and 2-propanol usually promote the formation of all types of adduct ions (Fig. 6). Table 1 briefly summarizes all observed fragment and adduct ions providing very similar patterns for all studied compounds. The summary of the observed ions for the particular studied compounds is shown in Table 1.

The negative ion spectra in the full-scan mode (Fig. 8(A)) and MS/MS of [M − H]$^-$ ion at $m/z$ 1987 (Fig. 8(B)) are depicted for compound **11**. Detailed interpretation of extended range of MS$^n$ spectra (not shown) provides a solid base for the proposal of fragmentation scheme presented in Fig. 9. All individual steps in the fragmentation scheme have been confirmed by appropriate MS$^n$ experiments. The most important ion in negative ion mass spectra is [M − H]$^-$ confirming the MW, which is subjected to subsequent MS$^n$ measurements (Fig. 8). It is important to note that the [M − H]$^-$ ion is observed only with the 'compound stability' tuning parameter decreased to 20%.

## CONCLUSIONS

The present work on the ESI-MS$^n$ measurements shows a great potential in characterizing and determining the structures of complex organometallic compounds containing many tin atoms. The comparison of the theoretically calculated and experimentally measured isotopic patterns is used for the determination of the number of tin atoms, in particular, fragment and adduct ions at least up to four tin atoms in individual ions, which simplifies the spectral interpretation. Significant differences are noted in the spectra of complex organotin compounds when different solvents (e.g. acetonitrile, methanol, ethanol and 2-propanol) are used for the direct infusion measurements. Alcoholic solvents form unusual adducts with organotin species, which is used as the supplementary information for the identification. To our best knowledge, the present paper is the first to deal with the detailed interpretation and structural characterization of organometallic compounds containing up to four tin atoms and $m/z$ values over 2000 Th, which should contribute to a better understanding of adduct formation process of complex organometallic compounds in the gas phase.

## Acknowledgements

This work was supported by projects No. MSM0021627502 (Ministry of Education, Youth and Sports of the Czech Republic), No. 203/05/2106 (Czech Science Foundation) and No. SR/S1/IC-03/2005 (TSBB, Department of Science and Technology, New Delhi, India).

## REFERENCES

1. Tiekink ERT. Structural chemistry of organotin carboxylates: a review of the crystallographic literature. *Applied Organometallic Chemistry* 1991; **5**: 1.
2. Lukevics E, Pudova O. Biological activity of organotin and organolead compounds. *The Chemistry of Organic Germanium, Tin and Lead Compounds* 2002; **2**: 1685.
3. Roesky HW, Haiduc I, Hosmane NS. Organometallic oxides of main group and transition elements downsizing inorganic solids to small molecular fragments. *Chemical Reviews* 2003; **103**: 2579.
4. Ebdon L, Hill SJ, Rivas C. Organotin compounds in solid waste: a review of their properties and determination using high-performance liquid chromatography. *Trends in Analytical Chemistry* 1998; **17**: 277.
5. Jones-Lepp TL, Varner KE, McDaniel M, Riddick L. Determination of organotins in water by micro liquid chromatography-electrospray/ion trap mass spectrometry. *Applied Organometallic Chemistry* 1999; **13**: 881.
6. Basu Baul TS, Singh KS, Holčapek M, Jirásko R, Linden A, Song X, Zapata A, Eng G. Electrospray ionization mass spectrometry of tributyltin(IV) complexes and their larvicidal activity on mosquito larvae; crystal and molecular structure of polymeric $(Bu_3Sn[O_2CC_6H_4\{N = N(C_6H_3\text{-4-OH}(C(H) = NC_6H_4OCH_3\text{-4}))\}\text{-o}])_n$. *Applied Organometallic Chemistry* 2005; **19**: 935.
7. Armelao L, Schiavon G, Seraglia R, Tondello E, Russo U, Traldi P. Electrospray ionization mass spectrometric study of the hydrolysis-polycondensation process of $Sn(OBu^t)_4$. *Rapid Communications in Mass Spectrometry* 2001; **15**: 1855.
8. Altmann R, Jurkschat K, Schürmann M, Dakternieks D, Duthie A. Methylene-bridged tri- and tetratin compounds as Lewis acids. *Organometallics* 1997; **16**: 5716.
9. Beckmann J, Henn M, Jurkschat K, Schürmann M. Hydrolysis of bis((trimethylsilyl)methyl)tin dihalides. Crystallographic and spectroscopic study of the hydrolysis pathway. *Organometallics* 2002; **21**: 192.
10. Basu Baul TS, Masharing C, Willem R, Biesemans M, Holčapek M, Jirásko R, Linden A. Self-assembly of diorganotin(IV) 2-{[(E)-1-(2-oxyaryl)alkylidene]amino}acetates: An investigation of structures by X-ray diffraction, solution and solid state tin NMR, electrospray ionisation MS. *Journal of Organometallic Chemistry* 2005; **690**: 3080.
11. Basu Baul TS, Singh KS, Holčapek M, Jirásko R, Rivarola E, Linden A. Synthesis, characterization and crystal structures of polymeric and dimeric triphenyltin(IV) complexes of 4-[((E)-1-{2-hydroxy-5-[(E)-2-(2-carboxyphenyl)-1-diazenyl]phenyl}-methylidene)amino]aryls. *Journal of Organometallic Chemistry* 2005; **690**: 4232.
12. Basu Baul TS, Singh KS, Lyčka A, Holčapek M, Linden A. Synthesis of a cyclic dinuclear organotin carboxylate via simultaneous debenzylation and decarbonylation reactions: X-ray crystal structure of $[(PhCH_2)_2\{O_2CC_6H_4\{N(H) - N = (C_6H_3\text{-4(=O)-5-O)}\}\text{-o}\}Sn]_2$. *Journal of Organometallic Chemistry* 2005; **690**: 1581.
13. Růžička A, Lyčka A, Jambor R, Novák P, Císařová I, Holčapek M, Erben M, Holeček J. Structure of azo dye organotin(IV) compounds containing a C,N-chelating ligand. *Applied Organometallic Chemistry* 2003; **17**: 168.
14. Jambor R, Dostál L, Růžička A, Císařová I, Brus J, Holčapek M, Holeček J. Organotin(IV) derivates of some O,C,O-chelating ligands. *Organometallics* 2002; **21**: 3993.
15. Dakternieks D, Zhu H, Tiekink ERT, Colton R. Synthesis, structure and reactions of $[(BuSn)_{12}O_{14}(OH)_6]Cl_2.2H_2O$: solution studies using $^{119}$Sn NMR and electrospray mass spectrometry. *Journal of Organometallic Chemistry* 1994; **476**: 33.
16. Biesemans M, Duthie A, Jurkschat K, Verbruggen I, Willem R, Zobel B. Transients from a mixture of $[(R(O)Sn)_2C(CH_3)_2]_2$ and $(RCl_2Sn)_2C(CH_3)_2$ [R = $(SiMe_3)_2CH$]: an identification in situ by 1D $^{119}$Sn and $^{1}$H–$^{119}$Sn HMQC NMR spectroscopy and electrospray mass spectrometry *Applied Organometallic Chemistry* 2003; **17**: 298.
17. Pejchal V, Holeček J, Nádvorník M, Lyčka A. $^{13}$C and $^{119}$Sn NMR spectra of some mono-n-butyltin(IV) compounds. *Collection of Czechoslovak Chemical Communications* 1995; **60**: 1492.
18. Pejchal V, Holeček J, Lyčka A. $^{13}$C and $^{119}$Sn NMR spectra of some monophenyltin(IV) compounds. *Scientific Papers of the University of Pardubice Series* 1996; **A2**: 35.
19. Novák P, Padělková Z, Kolářová L, Císařová I, Růžička A, Holeček J. Structure and properties of double-C,N-chelated tri- and diorganotin(IV) halides. *Applied Organometallic Chemistry* 2005; **19**: 1101.
20. Casas JS, Castiñeiras A, Couce MD, Jorge ML, Russo U, Sánchez A, Seone R, Sordo J, Varela JM. Triphenyltin(IV) sulfanylpropenoates: synthesis, crystal structures and antimicrobial activities. *Applied Organometallic Chemistry* 2000; **14**: 421.
21. Kellö E, Vrábel V, Skačáni I. Tris(N,N-diethyldithiocarbamato-S,S')phenyltin. *Acta Crystallographica* 1995; **C51**: 408.
22. Traeger JC. Electrospray mass spectrometry of organometallic compounds. *International Journal of Mass Spectrometry* 2000; **200**: 387.
23. Wei J, Miller JM. Electrospray ionization mass spectrometry of tribenzyltin substituted-phenoxyacetate coumpounds. *Journal of Mass Spectrometry* 2001; **36**: 806.
24. Lawson G, Dahm RH, Ostah N, Woodland ED. Electrospray mass spectrometry: an alternative method for the identification of organotin compounds. *Applied Organometallic Chemistry* 1996; **10**: 125.
25. Henderson W, Taylor MJ. Organotin halides and their hydrolysed species studied in solution by positive and negative ion electrospray mass spectrometry. *Polyhedron* 1996; **15**: 1957.
26. Kolářová L, Holčapek M, Jambor R, Dostál L, Růžička A, Nádvorník M. Structural analysis of 2,6-[bis(alkyloxy)methyl] phenyltin derivatives using electrospray ionization mass spectrometry. *Journal of Mass Spectrometry* 2004; **39**: 621.
27. Colton R, Traeger JC. The application of electrospray mass spetrometry to ionic inorganic and organometallic system. *Inorganica Chimica Acta* 1992; **201**: 153.
28. Xu X, Nolan SP, Cole RB. Electrochemical oxidation and nucleophilic addition reactions of metallocenes in electrospray mass spectrometry. *Analytical Chemistry* 1994; **66**: 119.
29. Holčapek M, Kolářová L, Růžička A, Jambor R, Jandera P. Structural analysis of ionic organotin(IV) compounds using

electrospray tandem mass spectrometry. *Analytical Chemistry* 2006; **78**: 4210.

30. Özkar S, Finke RG. The hydrogenphosphate complex of (1,5-cyclooctadiene)-iridium(I), $\{[Bu_4N](1,5\text{-}COD)Ir.HPO_4]\}_n$: synthesis, spectroscopic characterization, and ES-MS of a new, preferred precursor to $HPO_4{}^{2-}$ and $Bu_4N^+$ stabilized $Ir(0)_n$ nanoclusters. *Journal of Mass Spectrometry* 2004; **689**: 493.
31. Peveling K, Henn M, Duthie A, Löw Ch, Mehring M, Schürmann M, Costisella B, Jurkschat K. Mechanistic studies on the cyclization of organosilicon and organotin compounds containing the O,C,O-coordinating pincer type ligand $\{4\text{-t-Bu-2,6-}[P(O)(OR)_2]_2\,C_6H_2\}^-$ ($R = i - Pr$, Et): phosphorus (POC)-versus carbin (POC)-attack. *Organometallics* 2004; **23**: 1501.
32. Meija J, Centineo G, Alonso JIG, Sany-Medel A, Caruso JA. Interpretation of butyltin mass spectra using isotope pattern reconstruction for the accurate measurement of isotope ratios from molecular clusters. *Journal of Mass Spectrometry* 2005; **40**: 807.
33. Basu Baul TS, Rynjah W, Rivarola E, Lyčka A, Holčapek M, Jirásko R, de Vos D, Butcher RJ, Linden A. Synthesis and characterization of bis[dicarboxylatotetraorganodistannoxane] units involving 5-[(E)-2-(aryl)-1-diazenyl]-2-hydroxybenzoic acids: an investigation of structures by X-ray diffraction, NMR, electrospray ionisation MS and assessment of in vitro cytotoxicity. *Journal of Organometallic Chemistry* 2006; **691**: 4850.

DOI: 10.1002/jms